Available online at www.sciencedirect.com
ScienceDirect
Catalysis Today 129 (2007) 391–396
CATALYSIS TODAY
www.elsevier.com/locate/cattod

The role of carbon deposition on precious metal catalyst activity during dry reforming of biogas

Federico Barrai, Tracy Jackson, Noah Whitmore, Marco J. Castaldi *

Earth & Environmental Engineering Department (HKSM), Columbia University, NY 10027, United States

Available online 24 October 2007

Abstract

A preliminary investigation into the dry reforming (synthesis gas production) of landfill gas (LFG) was performed using precious metal catalysts. Thermogravimetric analysis work was performed on the dry reforming reaction over 0.5% Pt/γ-Al_2O_3 catalysts. Variables such as reforming temperature, CO_2 concentration, and the effect of pre-reduction have been studied. It was found that reforming at 900 °C with pre-reduction gave the most H_2 production for reactant gas concentrations similar to LFG. However, at this high temperature there was significant weight gain measured. EDX analysis and follow up oxidation tests confirmed that it was due to carbon deposition on the catalyst surface. Yet, this weight gain, up to 24% in some cases, did not coincide with a decrease in catalyst activity as was the case for the lower temperature tests. One possible mechanism for this is the onset of the carbon gasification (Boudouard) reaction at high temperatures. For increased CO_2 concentrations, the activity of the catalyst at high temperatures was maintained (high production of syngas) despite significant carbon deposition.

Keywords: Greenhouse gas reforming; Carbon formation; TGA

1. Introduction

As global energy demands increase, more consideration will be given to the future of energy supply. With the ultimate goal to develop a hydrogen economy, attention has recently been given to H_2 production from all sources. This has led to the increasing study of the dry reforming of methane focusing on the development of catalysts which exhibit high activity and stability [1,2]. One emergent area in particular is the use of biogas produced from anaerobic decomposition of organic material. This biogas typically contains equal amounts of CH_4 and CO_2, which if reformed properly can provide a renewable source of hydrogen essentially from waste [3]. Landfills are currently the largest source of this biogas in that they decompose municipal solid wastes anaerobically and landfill gas to energy (LFGTE) projects that directly combust the LFG are being implemented.

Landfills are also the largest source of U.S. methane emissions and they have emitted approximately 37 to 57 million tonnes of methane or 13–20% of the total U.S. methane emissions in 2006 [5,6]. Municipal Solid Waste (MSW) landfills generate 93% of U.S. landfill methane emissions. Over 2500 landfills currently operate in the U.S. [7] The 1996 Clean Air Act requires the reduction of methane emissions from landfills. Landfill methane emissions can be reduced through methane recovery and use projects (e.g. landfill gas to energy – LFGE), as well as flaring. Currently, only about 330 U.S. landfills have methane utilization projects out of 600 candidate landfills [5]. The recovered methane is used as on-site fuel to generate electricity, or sold to energy end-users [5,8,9].

The CO_2 and CH_4 from the landfills are ideal candidates for reforming reactions that yield either; (i) synthesis gas (CO and H_2) [10], to be used directly to enhance the combustion performance of various systems or (ii) high value products such as ethylene [10,11]. These reforming reactions are endothermic and as such require substantial amounts of energy to drive them. The implementation of the right catalytic reactor will overcome this contraint by combining exothermic reactions and selectivity to provide the necessary energy and promote the desired reforming reactions. The ideal scenario then would be to operate the reforming reactions in an autothermal mode where heat released, via exothermic reactions, provides the necessary energy to drive the desired endothermic reactions. One way to do this is to mix the CO_2/CH_4 feed with air or oxygen resulting in a fuel-rich

* Corresponding author.
E-mail address: mc2352@columbia.edu (M.J. Castaldi).

0920-5861/$ – see front matter © 2007 Elsevier B.V. All rights reserved.
doi:10.1016/j.cattod.2007.07.024

mixture where a precise amount of oxygen consumes CH_4 to generate the heat needed to drive the reforming reaction between CO_2 and the partial oxidation products, particularly H_2 and any remaining CH_4. This type of metered autothermal reactor has been developed by many groups [12], yet has not been applied to greenhouse gas reforming to our knowledge. The following reactions show the predominant routes to converting methane to syngas and the carbon formation reaction in the presence of significant amounts of CO. Reaction (3) is the dry reforming reaction and reactions (2) and (3) combined would constitute the autothermal reforming reaction sequence.

$$CH_4 + H_2O \leftrightarrows CO + 3H_2 \qquad \Delta H = +226\,\text{kJ/mol} \tag{1}$$

$$CH_4 + 1/2O_2 \rightarrow CO + 2H_2 \qquad \Delta H = -44\,\text{kJ/mol} \tag{2}$$

$$CH_4 + CO_2 \leftrightarrows 2CO + 2H_2 \qquad \Delta H = +261\,\text{kJ/mol} \tag{3}$$

$$2CO \leftrightarrows CO_2 + C \qquad \Delta H = -173\,\text{kJ/mol} \tag{4}$$

In the case of dry reforming (3), both reactants are inexpensive, are greenhouse gases, and become resources instead of undesired emissions. It is this dry reforming process that is perfectly suitable for conversion of LFG to syngas. However, because this process essentially entails stripping hydrogen from methane and oxygen from carbon dioxide, there is a significant potential for carbon formation to occur and deposit on the catalyst surface [13–15]. Many researchers that studied dry reforming did so using transition metal complexes and formulations and found carbon formation on the surface to be an issue [8,15–25]. As carbon formation is a process which occurs during catalyst operation, it is essential to understand the mechanism by which coke is formed with respect to a particular catalyst and temperature regime. A calculation of the thermodynamics of the dry reforming reaction indicate that carbon is favored at temperatures below 800 °C, yet during the actual operation, product formation is a competition between thermodynamics and kinetics. Under the umbrella of carbon deposition, there are multiple types including atomic carbon, amorphous carbon, bulk carbide, and crystalline graphitic carbon which any one or combination of types can impact the catalyst.

Due to economics, the use of Ni catalysts has been common in past studies, but carbon deposition has been shown to be less significant on precious metal catalysts. As the importance of greenhouse gas reduction continues to escalate, the cost of the catalyst will become less significant, leaving a primary need to find the most effective catalyst.

In the 1960s, Bodrov et al. published a series of works on steam reforming and dry reforming using nickel catalysts [26,27]. In the early 1990s there was a renewed interest in this reaction because it was shown that noble metal catalysts were not as prone to carbon deposition as was the nickel (which ultimately leads to a longer lifetime of the catalyst) and they provided high catalytic activity. Due to the potential that an effective catalyst could lead to significant greenhouse gas mitigation, in particular CO_2, work has continued on many fronts.

The metal catalysts that have been studied thus far for dry reforming are Ni, Rh, Pt, Pd, Re, Ir, and Ru. Rostrup-Nielsen and Bak Hansen studied various precious metals supported on MgO and found that replacing steam with CO_2 in the reforming reactions leads to a decrease in activity and the extent of which depends on the metal used. They deduced that Ru and Rh demonstrate the highest activity for dry reforming [23]. In addition, Rostrup-Nielsen and Bak Hansen found that the rate of carbon formation was far less for the noble metals than for nickel. They found no carbon formation on Ru and Rh, rapid formation on Pd above 600 °C, and slow formation on Ir and Pt above 750 °C. They predicted that the source of the carbon was methane decomposition [23].

Cornaglia et al. studied Rh and Pt supported on La_2O_3 in a membrane reactor. They varied the metal loading and found that the higher the metal loading, the higher the conversion of methane and carbon dioxide. They were able to achieve conversions higher than thermodynamically predicted [17]. Although there was no evidence of carbon deposition through the TGA work performed by Cornaglia for Rh and Pt, Laser Raman spectroscopy detected a small amount of graphitic carbon on the surface of the catalysts after 100 h on stream. However, the researchers did not indicate that this carbon could account for the decreased conversion on the Pt after 24 h on stream [17].

Claridge et al. found that Re displays activities and selectivities comparable to Ru, Rh, and Ir. These metals were supported on γ-alumina with the loading of the Re being five times that of the other metals. However, Re only displayed high conversion and selectivities to CO at high temperatures (>900 K) while the noble metals gave near equilibrium conversions and selectivities over the entire temperature range (873–1073 K) [28]. During Claridge's investigation into the activity of Re, he found there to be no detectable carbon deposition on Re, and he suggests that the rate of carbon deposition for Re is equivalent to Ru and Ir [28].

Richardson et al. studied Rh and Pt–Re supported on γ-Al_2O_3 and found that even when Re was added to Pt/γ-Al_2O_3, Rh still exhibited a higher activity. The Pt/Re mass ratio of 0.25 gave equivalent stability but with less activity [21].

Based on the above literature, this leads to the motivation for this investigation. While Pt is not the most active catalyst for the dry reforming reaction, it has the highest resistance to carbon formation leading to stable performance. Furthermore, to date there has not been a systematic TGA study of Pt to understand the kinetics and parameters associated with carbon formation for dry reforming.

2. Experimental

All reactions were performed in a simultaneous TG-DTA/DSC Apparatus STA 409PC/4/H *Luxx* manufactured by Netzsch. The gases delivered to the TGA were metered using rotameters by Matheson Tri-Gas (model FM1050 with a flow range in air of 0–150 ml/min) and Gilmont (model GF1010 with a flow range in air of 0.2–90 ml min^{-1}). The product gases from the TGA reactions were analyzed using the 4 channel Agilent 3000 Micro Gas Chromatograph (MicroGC). All of the tubing was 1/4 in. Teflon® tubing and the connectors were

stainless steel Swagelok. It should be noted that the product concentrations are low due to dilution from a nitrogen sweep gas that is required to ensure stable TGA operation.

The reactant gases (CH_4, CO_2, H_2, with a balance of N_2) were all certified UHP grade. They are fed to the system through calibrated Gilmont and Matheson flowmeters. The Matheson flow meter is used solely for the protective gas for the TGA, and in this set up was set to 20 ml min^{-1} N_2 for all runs. The gas flow rates were 7 ml min^{-1} for CH_4 and CO_2 and 90 ml min^{-1} for N_2 which included the protective gas flow. The reactant gases exit the Gilmont flow meters and are coupled to a manifold which enables a single feed to the TGA. Inside the TGA the reactant gases come in contact with the catalyst sample and are exposed to the temperature ramp for the test. The product gases from the experiment exit the TGA and travel to the MicroGC for on-line analysis. Catalyst samples were obtained from Engelhard Corporation in powder form containing 0.5% Pt on γ-Al_2O_3. Approximately 3 mg were placed into a 5 ml clean crucible for each experiment. Each time a catalyst was tested the complete experiment consisted of both a pretreatment step and a dry reforming step. For almost all of the tests, the temperature program was the same during the pretreatment and dry reforming steps, and any exceptions to this are indicated where appropriate. The temperature programs consisted of an initial ramping segment (all at 20 K/min) followed by an isothermal segment to allow for extended reaction time.

3. Results and discussion

3.1. Effect of pre-reduction

Fig. 1 shows the results from a TGA experiment using CH_4 and CO_2 in a nitrogen diluent. Mass change measurements show two distinct regimes over the entire range tested. A low to mid-temperature regime where the mass is relatively constant, this is the case for the entire collection of 500 °C and 700 °C experiments discussed below. The second major regime is where there is an abrupt mass decrease, which coincides with a peak in the activity, is followed by a gradual increase in mass as the activity levels off at the higher temperature, 900 °C. The onset of reaction occurs at 400 °C where H_2 and CO begin to form which coincides with a change in mass of the catalyst. The first regime is probably the reactants, methane, CO_2 or both, adsorbing on the surface and reacting to form syngas. The second regime is likely carbon formation on the surface due to catalytic cracking of methane. As shown in Fig. 1, shortly after the isothermal portion of the test is established, there is a rapid decrease in mass by about 2 to 3%, preceded by a slow increase. The mass increase up to the point of the near-step decrease in mass is due to methane and carbon dioxide adsorbing on the surface. The methane is likely dehydrogenating to form surface C and H_2 while the carbon dioxide molecule reduces to form surface CO and O [29]. The adsorbed C from the methane molecule then reacts with the O provided by the carbon dioxide molecule to form more surface CO. The rapid decrease occurs when both surface and reactant chemical species, and any molecules adsorbed at lower temperatures, quickly desorb as well as a significant reduction in additional adsorption from the gas phase. At 900 °C phase change (sintering) of the alumina support can be expected (see Table 1), which is accompanied by a slight drop in activity. Fig. 3 shows a plot of H_2 generation for a pure alumina sample, showing a constant H_2 generation for 100 min at 900 °C, without exhibiting evidence of deactivation.

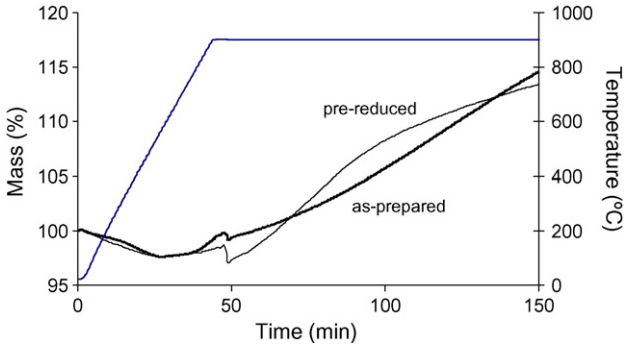

Fig. 1. Comparison of mass percent gain for pre-reduced and non-pre-reduced 0.5% Pt/γ-Al_2O_3 catalysts. Mass percent gain and temperature is shown as a function of time for an inlet stream of 7 ml CH_4, 7 ml CO_2, and 90 ml N_2.

The effect of the pre-reduction of catalysts has also been explored by comparing the carbon deposition and conversion of pre-reduced versus non-pre-reduced, or as-prepared catalyst samples (Figs. 1–3). To pre-reduce the catalyst, the sample was subjected to an atmosphere of 10% H_2 with a N_2 background and heated at a rate of 20 °C per minute until the temperature at which the subsequent dry reforming test would be done, for example 900 °C. Comparisons of conversion and mass percent growth could then be made for dry reforming runs between samples which had been pre-reduced and samples which were not subject to any pretreatment before the dry reforming, i.e. as-prepared. Fig. 1 also shows for the Pt catalyst that pre-reduced samples yielded a greater rate of carbon build up initially.

Table 1
BET surface area measurements for selected catalyst samples

Sample description	Surface area (m^2/g)
Fresh Al_2O_3 support	188
Fresh Pt catalyst	152
DR at 900 °C, as-prepared	159
DR at 900 °C, reduction at 900 °C	163

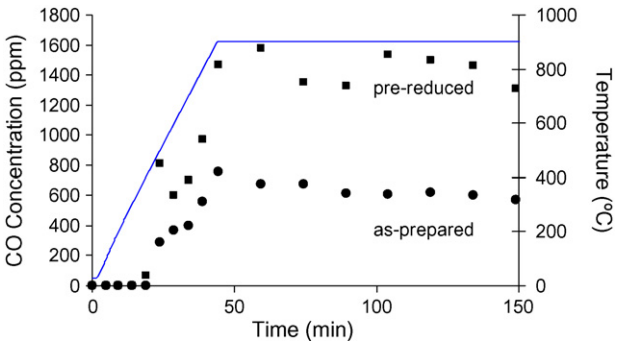

Fig. 2. Pre-reduced vs. as-prepared CO.

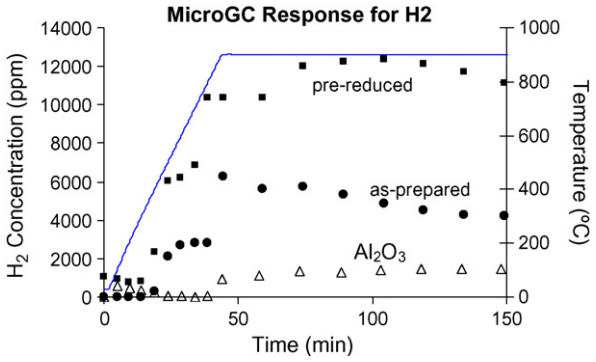

Fig. 3. H_2 conversion using pre-reduced and non-pre-reduced 0.5% Pt/γ-Al_2O_3 samples. Conversion is shown as a function of time and temperature for an inlet stream of 7 ml CH_4, 7 ml CO_2, and 90 ml N_2. Experiment on pure alumina (uncatalyzed) is shown for comparison.

Ultimately, however, both samples achieved nearly the same amount of mass gain. Typically, a reduction step serves to enhance dispersion of the catalyst metal and thus more catalytic sites would be exposed [2,14,30,31]. It may be the case that a higher percentage of exposed sites adsorb more reactants, thus leading to a higher rate of mass buildup. However, synthesis gas conversion from the pre-reduced catalyst was still greater by a factor of two from the as-prepared catalyst after 2 h at 900 °C (Figs. 2 and 3).

To ensure that the reactions observed were catalyzed by the precious metal, a test was done where only the un-catalyzed support was evaluated. Fig. 3 shows the results of the testing for hydrogen generation for the un-catalyzed support compared to the catalyzed samples for the same temperature profiles up to 900 °C. It is clear from the data that the un-catalyzed support had significantly less hydrogen production. In addition, not shown, there was no weight gain associated with the un-catalyzed support test. CO production resulted in a similar comparison as that for hydrogen generation, confirming the fact that there is no coke formation on the uncatalyzed support.

Figs. 2 and 3 show the production of CO and hydrogen, respectively, for a pre-reduced and as-prepared catalyst. It is clear that pre-reducing the catalyst enables it to be much more active for syngas generation. While the stoichiometry of the dry reforming reaction indicates that hydrogen and CO should be produced in a one-to-one ratio, it is consistently observed that hydrogen is produced in greater quantities. Typically it is about a 7.5:1 ratio in favor of hydrogen. The higher H_2 production is likely linked to carbon buildup on the catalyst surface. This is in line with a calculation of the rates of the two main possible reactions during the test, i.e. carbon deposition and dry reforming. Consider the carbon deposition step,

$$CH_4 + [S] \rightarrow C[S] + 2H_2 \quad (5)$$

This reaction has a nominal rate for C formation of 0.0015 min^{-1}, which can be calculated from Fig. 1. Therefore, a nominal H_2 production rate from reaction (5) is expected to be 0.003 min^{-1}. From Fig. 2 the total CO production rate can be calculated to be 4.3×10^{-5} min^{-1}. Under the assumption that the CO is only generated by the dry reforming reaction (3), the reformed H_2 rate is 0.00053 min^{-1} giving a total H_2 production rate of 0.00353 min^{-1}. This yields approximately 35 H_2 and 5 CO or nearly 7 to 1, which is very close to 7.5 to 1 concentration ratio observed. In addition, the equilibrium analysis shows, lower temperatures favor solid carbon during the reforming reaction. Thus at the lower temperatures tested, i.e. 700 °C and 500 °C, while there was considerably less activity, there was also very little CO observed.

Also of interest is the on-stream activity over time for the various tests. The pre-reduced tests consistently demonstrated steady activity over the time tested. The as-prepared samples, while there was less of a mass gain and lower overall activity, there was a reduction in activity during the isothermal portion of the tests. For example, Fig. 3 shows a steady decrease in activity for the as-prepared samples and higher level of activity for the pre-reduced samples. This may be related to the amount of dispersion of the active Pt metal, in that the higher dispersed samples have a sufficiently large amount of exposed sites to counter the increase in mass gain, that is likely due to carbon build up on the surface of the sites.

3.2. Effect of temperature

The effects of varying temperature on the dry reforming reaction have also been explored. While using pre-reduced Pt/γ-Al_2O_3 catalysts, carbon deposition and synthesis gas conversion was explored at temperatures of 500, 700 and 900 °C. Fig. 4 shows the results of the various temperatures vs. mass change. There is an initial decrease in mass, likely due to any moisture and adsorbed gases prior to the experiments followed by a slight increase for the 500 °C experiment, no mass gain for 700 °C and a significant increase in mass for the 900 °C tests (as seen in Fig. 1). In addition, the lower temperatures do not exhibit the rapid mass loss (near-step decrease of 2–3%) near 45 min that is seen for the high temperature experiment and discussed above. It is clear that temperature has an effect on whether the catalyst experiences that sharp mass loss followed by a rapid increase in mass gain. While the 900 °C experiment showed significant carbon deposition, it also exhibited the greatest CH_4 conversion, as seen in Fig. 5. At 700 °C and 500 °C, carbon deposition was respectively 56% and 83% lower than the deposition on the

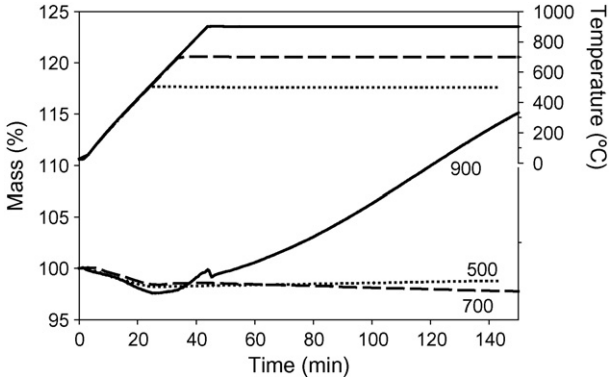

Fig. 4. The effects of varying temperatures for mass percent growth during dry reforming runs. Runs were performed on pre-reduced 0.5% Pt/γ-Al_2O_3 samples with inlet stream of 7 ml CH_4, 7 ml CO_2, and 90 ml N_2.

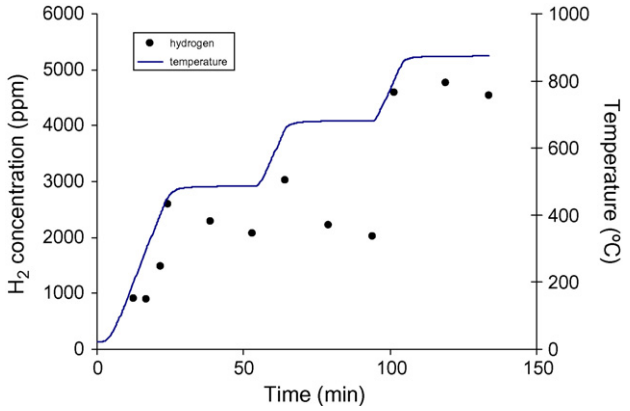

Fig. 5. Ramp and soak on activity showing the performance decrease at low temperatures and stable performance at high temperature.

catalyst at 900 °C. However, for the 900 °C sample, though it showed high H_2 and CO production, carbon was still increasing at the end of a 2 h isothermal run.

Fig. 6 plots the concentration of hydrogen produced versus time on stream in the TGA for the three temperatures tested with pre-reduced samples. For the first 29 min all three samples behave similarly as the temperatures are continuously increased. After approximately 30 min, which is near the 700 °C isothermal portion and already into the 500 °C isothermal portion, there is a decrease in activity which persists for the remaining test time. Yet, in the test where 900 °C is the maximum isothermal temperature, there is a continued increase in activity followed by a constant performance during the isothermal portion of the test, until the activity decreases slightly towards the end of run-time.

3.3. Effect of CO_2 concentration

The effect of varying concentrations of CO_2 has also been studied preliminarily at temperatures of 700 °C and 900 °C and at CO_2:CH_4 ratios of 1, 2, and 4. At 900 °C, carbon deposition was greatest when the CO_2:CH_4 ratio was 4, next greatest at a ratio of 1, and lowest at a ratio of 2. The order of hydrogen production followed the same trend. At 700 °C, more carbon deposition occurred when the CO_2:CH_4 ratio was 2 than at a one-to-one ratio.

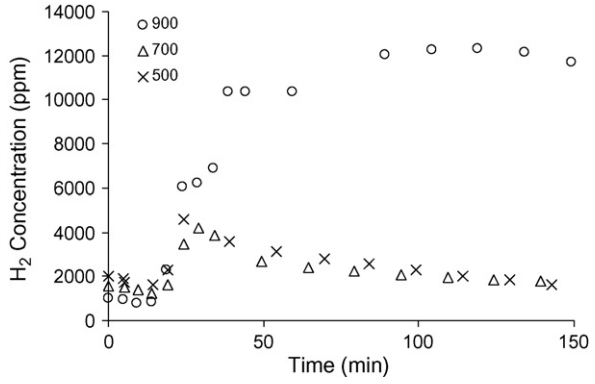

Fig. 6. H_2 conversion as a function of time for varying temperatures. Runs were performed on pre-reduced 0.5% Pt/γ-Al_2O_3 samples with inlet stream of 7 ml CH_4, 7 ml CO_2, and 90 ml N_2.

The above results and additional evidence provided by surface measurements discussed below suggest that while carbon formation is always favored thermodynamically, there is a competing kinetic effect. Since carbon deposition is present at all conditions it is possible that the carbon gasification reaction (reverse-Boudouard reaction) is responsible for the stable activity at high temperatures. As carbon is formed at the surface it can combine with reactant CO_2 to form CO, thus limiting the fouling effect the carbon buildup causes. Since the reaction is endothermic, at lower temperatures there is not enough energy to both initiate reforming and carbon gasification, however at high temperature there is sufficient energy.

3.4. Combined aging and temperature effect

Fig. 6 shows the results of an experiment done on a single pre-reduced catalyst sample where the temperature was increased to 500 °C, then held constant, increased again and held at 700 °C and finally increased and held at 900 °C. In effect this is a combination of aging and temperature effect on a pre-reduced catalyst sample. This test was done to separate the effects of aging due to time on stream versus the effect of mass gain. If deactivation of the catalyst was due to time on stream alone, it would be expected to be more severe as the test continues. It is clear that aging is occurring as evidence by the final concentration of hydrogen at the 900 °C isothermal portion compared to the hydrogen concentration in Fig. 6 for the 900 °C test. The most notable attribute of this experiment is the fairly constant performance of hydrogen at 900 °C versus a marked decrease in performance at 700 °C and 500 °C.

There is a reproduction of the mass gain conditions as was observed in Fig. 5. That is, the ramp and soak conditions up to an equal to 500 °C and 700 °C resulted in a very small mass gain, whereas on the ramp to 900 °C there was a substantial increase in the mass gain rate, nearly a factor of six. Again the only thing that can account for that increased mass gain is a carbon species adsorbing on the catalyst surface.

One of the dominant mechanisms of aging is loss of surface area during reaction or time on stream. Table 1 shows the results of BET measurements taken of the catalyst samples pre- and post-testing. As expected from the as-prepared, fresh support had the high surface area. The surface area of the catalyst after the platinum is applied is nearly the same as the post-tested as-prepared sample. This is the strongest evidence that there is no loss of surface area during the testing compared to a just calcined sample and therefore cannot be the mechanism by which the 500 °C and 700 °C samples lose activity. Moreover, these measurements support the observations that there is no aging due to sintering occurring on the catalyst sample at 900 °C, so it is unlikely it is occurring at lower temperatures. The final measurement in Table 1 shows the surface area of a pre-reduced sample after a test that exposed the catalyst to 900 °C. There the surface area is slightly higher than the as-prepared sample, which is expected, and was maintained during the testing. Although not shown, the BET measurements of the 500 °C and 700 °C samples were similar, which is expected since the testing occurred at lower temperatures.

The loss of activity at the 500 and 700 °C tests can only be attributed to either poisoning or fouling. Since the gases used were UHP, poisoning is not likely. Therefore, the evidence of mass gain during the experiments and the loss of activity due to fouling suggest carbon deposition on the catalyst surface. To determine the extent of carbon buildup, Energy Dispersive X-ray (EDX) Analysis was used on the post-tested samples that were exposed to the three temperatures of the study.

The EDX analysis on the sample used for the 900 °C experiment shows 22% carbon identified on the catalyst surface. This result correlates directly to the amount of mass gain during the 900 °C experiments. The EDX analysis at the lower temperatures showed very little if any carbon identified. In addition, the post-tested samples were re-run in the TGA in an air environment to oxidize the mass that was gained during the dry reforming experiments. The effluent of the TGA registered only carbon dioxide and air, further indicating only carbon was deposited on the surface. Finally, the amount of mass loss during the re-runs in air closely correlated to the weight gains obtained during the dry reforming experiments and the amount of carbon indicated by EDX analysis.

4. Conclusions

A series of TGA experiments were done on a $Pt/\gamma\text{-}Al_2O_3$ catalyst powder to determine the effect of carbon deposition on activity. Experiments at 500 °C and 700 °C showed less activity toward syngas production compared to 900 °C studies. Yet, observed mass gains were significantly higher in the 900 °C experiments. The 500 °C and 700 °C resulted in a mass gain of only few % while the 900 °C tests resulted in nearly 20% mass gain. This mass gain is attributed to carbon buildup on the catalyst surface and was verified using EDX analysis and post-testing in an air environment where the only product observed in the effluent was CO_2. Moreover, the 900 °C tests did not show an appreciable loss of activity during the testing as opposed to the lower temperature tests. The explanation for this could be that while carbon deposition is favored at all conditions, only at higher temperatures is there enough energy to initiate the boudouard reaction where the CO_2 in the reactant stream serves to gasify some of the carbon on the surface to CO.

Acknowledgements

The authors appreciate the support and discussion of Dr. Robert J. Farrauto during the work. In addition, the authors thank the NSF CTS program for partially supporting this under an SGER contract #CTS-05-53648. Finally, the authors wish to thank Velu Subramani for inviting them to present some of this work at the American Chemical Society's 1st Symposium on Hydrogen from Renewable Sources and Refinery Applications.

References

[1] S. Wang, G.Q. Li, G.J. Millar, Energy Fuels 10 (1996) 896.
[2] M.C.J. Bradford, M.A. Vannice, E. Ruckenstein, Catal. Rev., Sci. Eng. 41 (1999) 1.
[3] M. Aresta, A. Dibenedetto, I. Tommasi, Energy Fuels 15 (2001) 269.
[5] Environmental Protection Agency (EPA), Landfill Methane Outreach Program (LMOP), http://www.epa.gov/lmop, accessed 2006.
[6] N.J. Themelis, P.A. Ulloa, Renewable Energy 32 (2007) 1243.
[7] SCS Engineers, Comparative Analysis of Landfill Gas Utilization Technologies, Prepared for: North east Regional Biomass Program, CONEG Policy Research Center, Inc., Hall of the States, 400 North Capitol Street, N.W., Suite 382,Washington, D.C. 20001, File #0293066, March 1997.
[8] S. Kumar, S.A. Gaikwad, A.V. Shekdar, P.S. Kshirsagar, R.N. Singh, Atmos. Environ. 38 (2004) 3481.
[9] J. White, J. Robinson, Q. Ren, Waste Management, vol. 24, Amsterdam, Netherlands, 2004, p. 227.
[10] S.C. Tsang, J.B. Claridge, M.L.H. Green, Catal. Today 23 (1995) 3.
[11] W. Huang, K.C. Xie, J.P. Wang, Z.H. Gao, L.H. Yin, Q.M. Zhu, J. Catal. 201 (2001) 100.
[12] M.J. Castaldi, M. Lyubovsky, R. LaPierre, W.C. Pfefferle, S. Roychoudhury, SAE Technical Paper (2003).
[13] G. Avgouropoulos, T. Ioannides, C. Papadopoulou, J. Batista, S. Hocevar, H.K. Matralis, Catal. Today 75 (2002) 157.
[14] M.C.J. Bradford, M. Albert Vannice, Catal. Today 50 (1999) 87.
[15] J. Guo, H. Lou, H. Zhao, D. Chai, X. Zheng, Appl. Catal. A: Gen. 273 (2004) 75.
[16] J.N. Armor, Appl. Catal. A: Gen. 176 (1999) 159.
[17] L.M. Cornaglia, J. Munera, S. Irusta, E.A. Lombardo, Appl. Catal. A: Gen. 263 (2004) 91.
[18] J. Galuszka, R.N. Pandey, S. Ahmed, Catal. Today 46 (1998) 83.
[19] M.E.S. Hegarty, A.M. O'Connor, J.R.H. Ross, Catal. Today 42 (1998) 225.
[20] T. Inui, Appl. Organomet. Chem. 15 (2001) 87.
[21] J.T. Richardson, M. Garrait, J.K. Hung, Appl. Catal. A: Gen. 255 (2003) 69.
[22] J.R.H. Ross, Catal. Today 100 (2005) 151.
[23] J.R. Rostrup-Nielsen, J.H. Bak Hansen, J. Catal. 144 (1993) 38.
[24] M. Soick, O. Buyevskaya, M. Hoehenberger, D. Wolf, Catal. Today 32 (1996) 163.
[25] A.I. Tsyganok, M. Inaba, T. Tsunoda, K. Suzuki, K. Takehira, T. Hayakawa, Appl. Catal. A: Gen. 275 (2004) 149.
[26] N.M. Bodrov, L.O. Apel'baum, M.I. Temkin, Kinet. Catal. 5 (1964).
[27] N.M. Bodrov, L.O. Apel'baum, M.I. Temkin, Kinet. Catal. 8 (1967).
[28] J.B. Claridge, M.L.H. Green, S.C. Tsang, Catal. Today 21 (1994) 455.
[29] J. Wei, E. Iglesia, J. Catal. 224 (2004) 370.
[30] M.C.J. Bradford, M.A. Vannice, J. Catal. 183 (1999) 69.
[31] R.J. Farrauto, J. Catal. 41 (1976) 482.